



Published in final edited form as:

Ann Neurol. 2018 April ; 83(4): 816–829. doi:10.1002/ana.25212.

Neurochemical abnormalities in premanifest and early spinocerebellar ataxias

James M. Joers, PhD¹, Dinesh K. Deelchand, PhD¹, Tianmeng Lyu², Uzay E. Emir, PhD^{1,3}, Diane Hutter, RN¹, Christopher M. Gomez, MD, PhD⁴, Khalaf O. Bushara, MD⁵, Lynn E. Eberly, PhD², and Gülin Öz, PhD¹

¹Center for Magnetic Resonance Research, University of Minnesota, Minneapolis, MN 55455, United States

²Division of Biostatistics, University of Minnesota, Minneapolis, MN 55455, United States

³School of Health Sciences, Purdue University, West Lafayette, IN 47907, United States

⁴Department of Neurology, University of Chicago, Chicago, IL 60637, United States

⁵Department of Neurology, University of Minnesota, Minneapolis, MN 55455, United States

Abstract

Objective—To investigate whether early neurochemical abnormalities are detectable by high field magnetic resonance spectroscopy (MRS) in *individuals* with spinocerebellar ataxias (SCAs) 1, 2, 3 and 6, including patients without manifestation of ataxia.

Methods—A cohort of 100 subjects (N=18–21 in each SCA group, including premanifest mutation carriers; mean score on the Scale for the Assessment and Rating of Ataxia (SARA) <10 for all genotypes, and 22 matched controls) was scanned at 7 tesla to obtain neurochemical profiles of the cerebellum and brainstem. A novel multi-variate approach (distance-weighted discrimination) was used to combine regional profiles into an “MRS score”.

Results—MRS scores robustly distinguished individuals with SCA from controls, with misclassification rates of 0% (SCA2), 2% (SCA3), 5% (SCA1) and 17% (SCA6). Premanifest mutation carriers with estimated disease onset within 10 years had MRS scores in the range of early manifest SCA subjects. Levels of neuronal and glial markers significantly correlated with SARA and an Activities of Daily Living score in subjects with SCA. Regional neurochemical alterations were different between SCAs at comparable disease severity, with SCA2 displaying the most extensive neurochemical abnormalities, followed by SCA1, SCA3 and SCA6.

Interpretation—Neurochemical abnormalities are detectable in individuals prior to manifest disease, which may allow premanifest enrollment in future SCA trials. Correlations with ataxia and quality of life scores show that neurochemical levels can serve as clinically meaningful

Correspondence to: Gülin Öz, Center for Magnetic Resonance Research, University of Minnesota, 2021 Sixth Street Southeast, Minneapolis, Minnesota 55455, Tel: +1 612 625-7897, Fax: +1 612 626-2004, gulin@cmrr.umn.edu.

Author contributions. Study concept and design: CMG, KOB, LEE, GÖ. Data acquisition and analysis: JMJ, DKD, TL, UEE, DH, LEE, GÖ. Drafting the manuscript and figures: JMJ, GÖ. All authors read, critically revised, and approved the final manuscript before submission.

Potential Conflicts of Interest. Nothing to report.

endpoints in trials. Ranking of SCA types by degree of neurochemical abnormalities indicates that the neurochemistry may reflect synaptic function or density.

Disease-modifying treatments are in the pipeline for monogenic and fully penetrant neurodegenerative disorders thanks to advances in gene silencing strategies such as antisense oligonucleotides (ASO).¹⁻³ Safety and tolerability of intrathecal ASO therapy were demonstrated in familial ALS¹ and ASOs have recently shown remarkable efficacy in spinal muscular atrophy (SMA).² While these initial trials enrolled patients who already show symptoms of disease, mounting evidence argues for administration of such therapies in the earliest, including *premanifest*, stages of neurodegeneration.⁴ As reversibility of neurodegeneration is attenuated with progressing disease,^{5, 6} premanifest application of therapeutics facilitated by reliable detection of the earliest disease related cerebral abnormalities can enhance outcomes. Notably, a SMA trial is already enrolling presymptomatic patients with favorable interim findings.²

Premanifest abnormalities have been detected by neuroimaging in large cohorts with neurodegenerative diseases,⁷⁻⁹ however the modalities used in these studies currently have limited value in *individuals*.³ Magnetic resonance spectroscopy (MRS) enables non-invasive and regional quantification of endogenous neurochemicals¹⁰ and thereby may offer sensitivity to the earliest manifestations of neurodegeneration in the brain. We previously demonstrated that neurochemical abnormalities, reflecting neuronal loss or dysfunction (*N*-acetylaspartate [NAA], glutamate) and gliosis (*myo*-inositol), are detectable in spinocerebellar ataxias (SCAs) at *early* disease stage.¹¹⁻¹³ SCAs are autosomal dominantly inherited movement disorders characterized by degeneration of the cerebellum and its afferent and efferent connections.¹⁴ Progressive gait and limb ataxia is the predominant clinical manifestation and is widely monitored by the validated Scale for the Assessment and Rating of Ataxia (SARA).¹⁵ SCA1, SCA2, SCA3 and SCA6 are the most common genotypes accounting for more than half of the SCA patient population worldwide.¹⁴ They are caused by a CAG trinucleotide repeat expansion, and represent four of the nine known polyglutamine expansion disorders.¹⁶ Importantly, gene silencing strategies have shown efficacy with model systems of SCAs¹⁷⁻¹⁹ and intensive efforts are underway to translate these therapeutics to patients.

Evidence indicating neurochemical levels measured by MRS are likely to be sensitive to premanifest abnormalities in SCAs comes from transgenic mouse model studies in SCA1 that showed neurochemical abnormalities in the presymptomatic stage²⁰ and prior to overt pathological changes.²¹ Importantly, neurochemical alterations were also reflective of pathological progression²⁰ and reversal^{22, 23} in SCA1 models.

Therefore, our goal in this study was to measure the earliest neurochemical abnormalities in the cerebellum and brainstem in SCAs and to determine if neurochemical abnormalities are detectable at premanifest and early stages in individuals with SCAs. We further aimed to establish the clinical correlates of neurochemical abnormalities. Finally, we investigated the genotype-specificity of neurochemical abnormalities in these SCAs. To accomplish these goals, we studied the largest early-stage cohort of subjects with SCA1, SCA2, SCA3 and SCA6 for MRS investigations so far, including premanifest mutation carriers, and utilized

the highest sensitivity MRS methodology available to date at 7 tesla (T). We utilized a novel multi-variate approach (distance-weighted discrimination, DWD)²⁴ to combine regional profiles into an “MRS score” and hypothesized that the MRS score would provide a robust means by which to detect neurochemical abnormalities in the premanifest stage.

Methods

Study design

This was a cross-sectional observational study of early-stage subjects with SCA1, SCA2, SCA3 and SCA6 and age-range and sex-frequency matched healthy controls. Target enrollment was 20 subjects in each of the 5 groups. The study was powered based on our prior pilot data¹³ to provide sufficient power to detect overall differences in the major metabolites between groups within each of the 3 MRS volumes-of-interest (VOIs) with multiple comparisons correction for the 10 pairwise group contrasts of interest (see Statistical Analysis below). Effort was made to recruit patients with a SARA score¹⁵ 15 (range 0–40, 0 indicating no ataxia and 40 most severe ataxia) and with a similar SARA distribution between the 4 SCA groups, such that MRS data would be comparable between groups without the confounding effects of disease severity. A SARA score in the range 0–2.5 was considered the premanifest disease stage for participants with SCA and designates the stage prior to ataxia onset.²⁵ Since the expected age ranges for the patient groups were similar, one control group was deemed sufficient. Participants were scanned at 7T to obtain neurochemical profiles of the cerebellar vermis, cerebellar white matter and pons and were evaluated by the SARA scale within one day of MR scanning.

Participants

Subjects aged 20 to 75 years of age living in the United States and proximal regions of Canada were enrolled between March 2011 and September 2016. Genetically-confirmed individuals with SCA1, 2, 3, or 6 and controls were enrolled using the criteria described below. Fig. 1 provides an overview of subject census throughout the study.

SCA disease burden—A truncated version (*i.e.*, the first page) of the SARA form was administered remotely to assess disease burden; subjects with higher disease burden were excluded based on subject-supplied information regarding gait, stance and sitting and on evaluation of speech disturbance during a telephone conversation. Subjects whose truncated SARA score was 10 or lower (out of 24) were invited to participate.

Medical history—Subjects with diabetes were excluded due to possible confounds of oxidative tissue damage.²⁶ Individuals with known neurological disease or brain pathologies outside of SCA (*e.g.*, cancer, stroke) were excluded.

MR contraindications/limitations—Subjects with MR contraindications were excluded. Additionally, individuals with large head size (> 23-inch circumference) or a body mass index (BMI) > 40kg/m² were excluded due to accommodation limits of the MR hardware. Individuals who reported an inability to lie still for an hour, or those with claustrophobic tendencies, were excluded.

Lifestyle—Individuals with a history of tobacco or cannabis use were excluded due to possible confounds with neuronal oxidative damage²⁶ and/or neurochemical profile alterations.²⁷

Procedures

All procedures were approved by the Institutional Review Board: Human Subjects Committee of the University of Minnesota and informed consent was obtained from all participants. Volunteers were asked to discontinue antioxidant supplements for 3 weeks prior to the study since the most common supplemental antioxidants are eliminated over this time.^{28, 29} Subjects on benzodiazepine, antispasmodic and anti-Parkinson medications were requested to taper and hold the medication for 12–24 hours (depending on half-life of the specific medication) prior to the SARA assessment and MR scan to minimize possible confounds due to medication related alterations in neurotransmitter levels in the brain, in particular γ -aminobutyric acid (GABA). Anti-Parkinson medications are used to treat Parkinsonian symptoms in some SCA2 and SCA3 cases.

Clinical assessments—All subjects underwent the SARA assessment, which is a composite clinical scale with construct validity, internal consistency and inter-rater reliability¹⁵ and is based on inventories of gait, stance, sitting, speech disturbance, a finger-chase test, a nose–finger test, fast alternating movements and a heel–shin test. A quality of life score was obtained using the activities of daily living (ADL) portion of the Friedreich’s Ataxia Rating Scale.^{30, 31} Scores for this scale increase with poorer performance in aspects of speech, swallowing, cutting food, use of utensils, dressing, personal hygiene, falling, walking, sitting and bladder function and range from 0 to 36. Age of onset and age at diagnosis were based on self-reported information. Premanifest SCA subjects were assigned a missing age of onset.

MRI protocol—MR imaging and spectroscopy were performed using a 16-element volume RF transceiver³² on an actively-shielded Siemens 7T MR system operating under *Syngo* software release B17. Localized shimming of the RF transmit field, B_1^+ , was accomplished with additional hardware and software that permitted individual phase control of each of 16 individual 1kW RF channels, as previously described.^{33, 34}

A whole-brain, 1 mm isotropic 3D T_1 image (repetition time $TR = 2500$ ms, echo time $TE = 2.42$ ms, inversion time $TI = 1500$ ms, excitation flip angle = 5°) was used for MRS voxel placement. MR spectra were acquired from three VOIs, selected based on their known involvement in SCAs^{11–13}: cerebellar vermis ($10 \times 25 \times 25$ mm³), cerebellar white matter (CWM) ($17 \times 17 \times 17$ mm³), and pons ($16 \times 16 \times 16$ mm³) (Fig. 2). All spectra were acquired using a short-echo, semi-LASER sequence³⁵ ($TR/TE=5000/26$ ms, 64 transients), as described previously.^{36, 37} A series of unsuppressed water spectra was acquired at multiple echo times to estimate cerebrospinal fluid (CSF) contribution to the VOI.³⁶

Metabolite Quantification—The 64 individual spectra from each VOI were eddy-current, phase and frequency corrected prior to summation.^{36, 37} CSF voxel fraction was estimated from a biexponential fit to the intensities of the water spectra acquired from the TE series;

the T_2 of CSF was fixed at 565ms for this fit. Neurochemical profiles were quantified using LCModel³⁸ (version 6.3-0G) with water-scaling using previously published fitting parameters.³⁶ The basis set included model spectra for alanine (Ala), aspartate (Asp), ascorbate (Asc), glycerophosphocholine (GPC), phosphocholine (PC), creatine (Cr), phosphocreatine (PCr), γ -aminobutyric acid (GABA), glucose (Glc), glutamine (Gln), glutamate (Glu), glutathione (GSH), *myo*-inositol (mI), lactate (Lac), *N*-acetylaspartate (NAA), *N*-acetylaspartylglutamate (NAAG), phosphoethanolamine (PE), *scyllo*-inositol (sI), taurine (Tau) and experimentally obtained macromolecules and was generated as previously described.^{36, 37} For each VOI, metabolites with mean Cramér-Rao lower bounds (CRLB)

20% (estimated error of metabolite quantification) for any of the SCA cohorts or for controls were included in the statistical analyses. All concentrations except those for which the fitting failed and standard deviation (SD) could not be estimated (designated with a CRLB of 999% in LCModel) were used when calculating mean CRLBs for each cohort. For metabolites with strong correlations ($r < -0.7$), only the sum was reported, e.g. total creatine (tCr, Cr+PCr) and total choline (tCho, GPC+PC). Finally, Glu+Gln (Glx) and Glc+Tau was reported if one of the individual concentrations did not meet the mean CRLB 20% criterion in any of the 5 cohorts since these pairs of metabolites have similar spectral patterns and therefore tend to correlate with each other ($r < -0.5$).

Statistical Analysis

Group Comparison Analysis—Participant characteristics were compared among all groups using ANOVA for continuous characteristics (reporting Tukey corrected p-values for multiple comparisons) and chi-square test for sex (reporting Holm corrected p-values for multiple comparisons); Holm's correction is a Bonferroni step-down technique. For each VOI and each metabolite, concentrations were compared between groups using a general linear model with covariates for group, age, and sex. Tukey's method was applied to correct type I error for the set of all pairwise group comparisons. Then Holm's correction was applied within VOI to the Tukey-corrected p-values of group differences for the multiple testing across the metabolites.

Classification Analysis—Approaches by which to reduce dimensionality of data features (e.g., multi-region metabolite concentrations) or to weigh them by importance should facilitate group discrimination and visualization. We chose DWD based on its ability to handle high dimensionality and low sample size, a common limitation in biomedical imaging,²⁴ especially in the study of rare diseases. Here, we performed binary classifications for each pair of groups (Table 1), resulting in ten separate DWD analyses. The DWD-based "MRS score" is a measure of how far the subject's metabolite pattern is from the group-separating hyperplane. Misclassification was quantified using leave-one-out cross-validation. Separately for each VOI, we imputed metabolite concentrations where they were missing or where they had CRLB=999% by a random draw from a normal distribution with mean equal to the metabolite's mean and the SD equal to the metabolite's SD. The mean and SD were calculated excluding concentrations with CRLB=999% or with absolute CRLB greater than 2 SDs away from the group mean. Subjects with missing data included 0 SCA1, 3 SCA2, 6 SCA3, 1 SCA6, and 4 controls for the pons and 1 SCA3 and 1 SCA6 for the CWM.

Correlation Analysis—Using SCA participants only, Pearson’s correlation between clinical measures (SARA, ADL, disease duration) and DWD-based MRS scores (from the models of each SCA vs. controls) was computed by SCA group to see whether participants with more severe clinical measures tended to have metabolite patterns that were farther from the hyperplane. Holm’s type I error correction was applied per SCA group to account for the multiple testing of these correlations. Again using SCA participants only, Pearson’s correlation was computed between clinical measures and (non-imputed) metabolite concentrations per VOI; Holm’s correction was applied per SCA group per VOI.

Results

Participant enrollment and cohort characteristics

We enrolled genetically confirmed subjects with early (target SARA ≤ 15) including premanifest (SARA ≤ 2.5) SCA1, SCA2, SCA3 and SCA6, and age and sex frequency-matched controls meeting the eligibility criteria for cross-sectional scanning at 7T. Of the 341 subjects with SCA initially screened, 234 were excluded based on eligibility criteria and 30 declined, resulting in 84 enrolled subjects; of these, 78 had a successful scan, passed data quality measures, and were included in the final analysis (Fig. 1). Twenty-five control subjects were enrolled, resulting in 22 available for the final analysis. The control group was well-matched to all SCA groups with respect to age, sex, and BMI (Table 1). Among SCAs, age at enrollment, onset and diagnosis was higher for SCA6 than the other SCA groups. However, the SCA groups were well-matched for disease duration, SARA and ADL scores, demonstrating that our goal to match the genotypes for disease severity was achieved. In addition, the recruitment goal for cohorts with early SCA was achieved, with an average SARA score for each SCA group of less than 10. Specifically, remote screening with a truncated SARA resulted in most subjects having SARA within the target of ≤ 15 and only 3 subjects with SCA2 and 5 subjects with SCA6 having SARA above this range.

Neurochemical abnormalities in SCA1, 2, 3 and 6

MR spectra of high quality were obtained from the three target VOIs in all subject groups such that neurochemical differences in spectra from individual subjects with SCA vs. controls were visually apparent. Notably, neurochemical abnormalities, such as lower NAA were evident even in subjects at the premanifest stage (Fig. 2). Spectral quality, as evaluated by linewidth and signal-to-noise ratio (SNR), was comparable between the 5 groups, except for lower SNR in the vermis and pons in SCA2 and lower SNR in the vermis in SCA6, which was due to atrophy resulting in higher CSF contribution to the VOI. The spectral quality allowed the quantification of more than 10 metabolites that met the pre-defined reliability criteria (mean CRLB $\leq 20\%$) in each VOI (Fig. 3). Comparison of neurochemical profiles performed separately for each of these VOIs revealed significant neurochemical alterations in each SCA genotype compared to healthy controls (Table S1). Significant alterations in neurochemical profiles in the SCA groups vs. controls included lower NAA, a marker of neuronal integrity, higher mI, a putative glial marker, as well as alterations in other metabolites associated with cellular energetics (tCr, Glc), antioxidant capacity (Asc, GSH) and neurotransmission (Glu, Gln, GABA) in select VOI and with different patterns

among genotypes. Of these, Glu also serves as a neuronal marker due to its primary localization to neurons³⁹ and tCr may also mark gliotic activity.⁴⁰

Detection of neurochemical abnormalities at the premanifest stage

We first investigated the ratio tNAA/mI, which was previously shown to reliably distinguish patients with SCA1 from controls¹¹, for its ability to distinguish patients with all SCA genotypes from controls. The ratio distinguished SCA1, SCA2 and SCA3 cohorts from controls well in all 3 VOI and SCA6 cohort from controls moderately well in vermis and CWM data. The SCA cohorts included 9 premanifest mutation carriers (SARA range 0 – 1.5) and we noted that a majority of the premanifest subjects had tNAA/Ins ratios in the range of early manifest subjects, beyond one SD of control means (Fig. 4), consistent with neurochemical abnormalities that were visible in spectra acquired from these subjects (Fig. 2).

Next, we utilized a novel multi-variate approach, DWD, to investigate how successfully each SCA cohort was distinguished from controls by *combined* neurochemical data from the 3 VOI. DWD is a machine learning pattern-recognition algorithm; it finds an optimized hyperplane in high dimensional space that separates two or more groups based on minimizing the average inverse distance to the separating hyperplane. The distance from the separating hyperplane was then used as an MRS score combined across-metabolites and -regions for each participant. SCA1, SCA2 and SCA3 cohorts were distinguished from healthy controls almost perfectly (Fig. 5A), with a 0–5% misclassification rate (0% for SCA2, 2% for SCA3 and 5% for SCA1), while SCA6-control classification had a higher number of misclassified individuals (17%). We repeated the SCA6-control classification including age and sex as additional predictors and the results were unchanged. Importantly, 6 of the 9 premanifest individuals were classified with the manifest patients in the binary DWD analyses vs. controls (Fig. 5A).

To investigate if an ability to detect neurochemical abnormalities was related to how far from disease onset the subjects were, we estimated their time to onset using a recently developed statistical model.⁴¹ The premanifest mutation carriers who were classified by DWD as SCA had estimated time to onset of 10 years or less (Fig. 6), indicating that neurochemical abnormalities may be detectable up to 10 years before onset of ataxia.

Clinical correlations

To determine if MRS-measured metabolites may provide clinically meaningful endpoints in future ataxia trials, correlations between MRS scores (obtained from the comparisons to the control group) and the clinical measures of SARA score, ADL score, and disease duration were investigated for each SCA group (Fig. 7A, Table S2). MRS scores strongly correlated ($r > 0.60$) with SARA scores for SCA1 ($p < 0.01$, type I error corrected) and SCA2 ($p = 0.001$), and with disease duration ($p = 0.004$) and ADL ($p = 0.001$) for SCA2. MRS scores for SCA3 did not show correlations with these clinical measures, while MRS scores correlated with ADL for SCA6 ($p = 0.02$). To address the possibility that correlations between clinical measures and individual neurochemicals in select VOI may be missed when the DWD-based MRS scores, which combine information from all regions and neurochemicals, is utilized,

we also investigated correlations between clinical measures and select neurochemical concentrations. For this analysis we focused on neurochemicals that were shown to be correlated with SARA in prior work,^{11, 12} specifically two neuronal (tNAA, Glu) and two putative glial markers (mI and tCr). This analysis revealed correlations between individual neurochemical levels and clinical measures for all SCAs (Fig. 7B, Table S3). Notably, the glial marker mI in the CWM was strongly associated with ADL in SCA1. Strong correlations ($|r|>0.60$) were observed in SCA2 between neuronal markers in the vermis and pons and each of SARA and ADL, while they were limited to a glial marker in the pons for SCA3 and to a neuronal marker in the CWM for SCA6.

MRS based classification of SCA1, 2, 3 and 6

Lastly, we investigated if neurochemical profiles were different between different SCAs. Comparison of regional neurochemical profiles revealed significant differences between the SCA genotypes (Fig. 3, Table S1). Neurochemical abnormalities were most severe in SCA2, based on fractional differences in NAA, mI, Glu and tCr from controls and p-values. Pontine neurochemical levels were normal in SCA6. Consistently, highly statistically significant differences were observed in the pons between SCA6 and other SCAs, but also in the vermis and CWM (Table S1). Finally, neurochemical differences between SCA1 vs. SCA2 and SCA2 vs. SCA3 were highly significant, while SCA1 and SCA3 were not distinguished appreciably by neurochemical levels in the 3 VOI. Next, we utilized DWD analyses to investigate how successfully each SCA cohort is distinguished from each other when all regions and metabolites are used. Consistent with the neurochemical comparisons, SCA6 was well distinguished from other SCA genotypes, with 7–8% misclassification rates (Fig. 5B). SCA3 was distinguished reasonably well from SCA2, while it was more challenging to distinguish SCA1 from SCA2 and SCA3. The top 5 neurochemicals that drove the successful binary classifications included NAA and N-acetylaspartylglutamate (NAAG), as well as other reliably quantified neurochemicals, such as Glc+Tau, Glu and tCho (Table S4). While NAA and NAAG measurements in the vermis were prominent contributors to the separation of SCA groups from controls, neurochemical levels in the pons and CWM primarily distinguished the SCA groups. Specifically, neuronal markers NAA, NAAG and Glu in pons and CWM were critical in distinguishing SCA2 and SCA3 from SCA6, while NAA, NAAG in the pons, as well as putative glial marker Gln in CWM and GABA in vermis were important to distinguish SCA1 from SCA6. The SCA2-SCA3 separation was driven by neurochemicals in all 3 VOI, including NAA, NAAG and Glc+Tau.

Discussion

Here we report that neurochemical abnormalities are detectable by ultra-high field MRS in premanifest carriers of common SCA mutations whose *estimated* disease onset is within 10 years. We introduce the use of a novel multi-variate approach, DWD, to combine multi-regional neurochemical profiles into one score that can be compared to clinical measures. Significant correlations between DWD-based MRS scores and clinical measures were observed for SCA1, SCA2 and SCA6. In addition, clinical correlations were detected for select regional neurochemical levels in all SCAs. Importantly, we report associations between levels of neuronal and glial markers and a quality of life measure (ADL) for SCA1,

SCA2 and SCA6. Finally, regional neurochemical alterations were different between the four common SCAs at similar disease severity and allowed discrimination of the genotypes.

We were able to recruit a cohort of 100 subjects, a cohort size comparable to prior multi-site MRI studies in the common SCAs,⁴² at a single site. We targeted an early-stage SCA cohort because these patients are the most likely candidates for future clinical trials that would aim to intervene prior to substantial neurodegenerative changes. Each SCA cohort also included subjects in the premanifest stage, such that their neurochemical levels could be compared to the neurochemical abnormalities in a sizable manifest cohort. The study provided critical experience with recruitment for future trials. Namely, a cohort about 4 times the target sample size needs to be screened (Fig. 1) to recruit patients within the 0–15 SARA range and who are eligible for MRI. The use of the truncated SARA assessment remotely was successful in achieving an aggregate disease burden consistent with our target. However, the fact that some subjects were above the target SARA range of 0–15 also showed that our remote screening procedure, partly based on self-reporting, is susceptible to underestimation of disease burden. Finally, an important distinction of this study relative to prior MRI and MRS studies in SCAs was that we matched the sample size and disease severity between the SCA cohorts such that an ability to detect neurochemical abnormalities or correlations with clinical measures was not driven by a difference in sample sizes or disease burden between cohorts.

This study demonstrates the feasibility of detecting neurochemical abnormalities in individuals in the premanifest stage of SCAs. Neurochemical abnormalities in the premanifest stage of SCAs have been largely unexplored,²⁵ except for one report of altered NAA-to-creatine ratio in two asymptomatic SCA1 carriers.⁴³ The sensitivity of MRI to premanifest abnormalities has been shown in another polyglutamine disease, Huntington's disease,^{7, 9} however no MR modality has so far shown sufficient sensitivity to reliably detect pre-degenerative abnormalities in individuals.³ Similarly, the only large cohort study of MRI abnormalities in at risk individuals with the common SCAs⁸ showed morphometric differences in SCA1 and SCA2 mutation carriers vs. non-carriers in group analyses. Detection of neurochemical abnormalities by MRS may allow recruitment of those premanifest patients who are closer to disease onset in future SCA trials. While time to disease onset can be estimated based on current age and CAG repeat size,⁴¹ clinical manifestation can vary greatly amongst individuals with the same mutation,^{44, 45} therefore objective measures of cerebral disease at the premanifest stage are critical. Importantly, the neurochemical abnormalities were also apparent by evaluation of neurochemical levels/ratios in premanifest patients (Fig. 4), however the DWD-based MRS scores allowed a simple comparison of combined neurochemical abnormality to estimated time to disease onset. These data suggested that abnormalities in neurochemical profiles appear by as much as 10 years prior to ataxia onset, in agreement with recent observations of neurochemical changes that precede gross pathological alterations²¹ and ataxia onset²⁰ in SCA models. Longitudinal monitoring of our premanifest participants for ataxia onset will ultimately establish if neurochemical abnormalities are detectable 10 years prior to onset. Also, because the DWD-based MRS score is specific for a particular dataset, as is true for any predictive statistical model, a sufficiently large premanifest and manifest MRS sample,

preferably multi-site, will need to be accumulated to train the DWD model for utility of this score in future trials.

While investigating the rich neurochemical information provided by high field MRS provides insights into regional biochemical and cellular composition, there are advantages of combining the high dimensional MRS data into one score for enhanced clinical utility. We used the DWD approach because it provides better performance than other similar classification approaches based on high-dimensional inputs (such as support vector machines, which can have the ‘data piling’ problem²⁴), because it does not depend on multivariate normality in the high-dimensional input space for optimal performance (such as principal component analysis), and because the DWD output provides a ranking of data features that drive group classifications, thereby preserving the connection to the underlying neurochemical information. Using this approach, the discrimination of all SCA groups from controls, and that of SCA6 from SCA1, SCA2 and SCA3 was very successful, while the SCA2-SCA3 classification was moderately successful (Fig. 5). Importantly, the successful classifications were driven by features that were found to be very significant in the metabolite comparison analysis (Fig. 3, Table S4). This relationship helps to verify the DWD approach and illustrates the usefulness of including more basic statistical approaches when using techniques that aim to operate in high dimensional space, but return results in low dimensional space. The successful separation of SCA6 from the other genotypes and its poorer separation from controls is consistent with a milder pathology in this pure cerebellar ataxia with sparing of the pons.⁴⁶ The poor classification of SCA1 from SCA2 and SCA3 would likely be improved by collecting neurochemical profiles from other VOI. For example, striatal dopamine transporter deficits have been demonstrated in subjects with SCA2 and SCA3,⁴⁷ but not SCA1,⁴⁸ suggesting the MRS of the striatum may better discriminate between these genotypes. MRS detected neurochemical abnormalities were most severe in SCA2 in all 3 regions, followed by SCA1 and SCA3 and finally by SCA6. Remarkably, the degree of synaptic loss in the cerebellum and brainstem is also most severe in SCA2, followed by SCA3, SCA1 and SCA6,^{46, 49} indicating that the neurochemical abnormalities detected in common SCAs by MRS may primarily reflect synaptic function or density.

This study established correlations of cerebellar and brainstem neurochemical levels with clinical measures at early disease stage for all common SCAs. By matching sample size and disease severity between the SCA cohorts, our goal was to allow a definitive comparison of the strength of these MRS-clinical correlations between the genotypes and infer associations between regional neuronal and glial abnormalities and symptomatology. First, the combined cerebellar/brainstem neurochemical abnormality burden, as quantified by the DWD-based MRS score, was strongly correlated with disease severity only in SCA1 and SCA2 and disease duration in SCA2. This suggests that the ataxia severity in SCA1 and even more so in SCA2 is a function of the combined cerebellar and pontine deficit and that this combined neurochemical abnormality is related to disease duration at early stage in SCA2. Consistently, the largest number of significant correlations between individual neurochemicals and SARA were detected in SCA2 (Fig. 7B). Second, the fact that the DWD-based MRS scores were not correlated with disease severity (SARA) and duration in SCA3 and SCA6 suggested that neurochemical correlates of disease were more regional in

these genotypes. Note that these correlations were detectable despite our limited SARA range and are expected to be stronger for cohorts that include participants with higher disease severity. These associations suggest that the ataxia symptoms are driven by glial pathology in CWM in SCA1, while they are driven by primarily neuronal pathology in the vermis and pons in SCA2. Glial pathology in the pons appears to be primarily associated with the ataxia symptoms in SCA3 and finally, neuronal pathology in the CWM is associated with the ataxia symptoms in SCA6. The detection of correlations between regional neurochemical levels with a quality of life score (ADL) in SCA1, SCA2 and SCA6 is significant as such functional measures are highly critical in trials as clinically meaningful endpoints.

A limitation of our study is the small sample size for premanifest patients, nonetheless we were able to reliably detect neurochemical abnormalities in these individuals. Our findings warrant further MRS studies dedicated to the premanifest stage in SCAs. The single voxel MRS approach was chosen to enable highest data quality and quantification of a neurochemical profile, including metabolites that are critical to the neurodegenerative disease process.¹⁰ The choice of a 7T scanner, which was made to maximize our ability to detect early neurochemical abnormalities, may be considered a limitation of the study due to limited access to 7T scanners in the clinical setting. However, the metabolites that drove group separations are detected with equivalent reproducibility at 3T and 7T in the cerebellum.³⁷ Therefore, the widely available 3T platform is appropriate for future investigations into early neurochemical abnormalities in SCAs. We have used a non-standard MRS sequence (sLASER) for optimal data quality and because this sequence has been rigorously validated for within- and between-site reproducibility^{36, 37, 50} and has been utilized in clinical cohorts, including SCAs.¹² Finally, while the inhomogeneous 7T T₁ structural images were not amenable to robust volumetric analysis in this study, it will be critical to use a multi-modal MR approach that combines structural and neurochemical information in future studies.

In conclusion, we showed that neurochemical abnormalities are detectable by MRS in mutation carriers of hereditary neurodegeneration prior to the clinical manifestation of motor symptoms. These neurochemical abnormalities appear genotype-specific and are associated with disease severity and quality of life measures. Therefore, they may help identify subjects who are closest to clinical disease onset and provide clinically meaningful endpoints in upcoming trials, in particular those based on gene silencing strategies.

Supplementary Material

Refer to Web version on PubMed Central for supplementary material.

Acknowledgments

We thank the participants in this study, members of the US Clinical Research Consortium for Studies of Cerebellar Ataxias (CRC-SCA) for referring participants to our study and the staff of the Center for MR Research for maintaining and supporting the MR system. This work was supported by the National Institute of Neurological Disorders and Stroke (NINDS) grants R01 NS070815 and R01 NS080816 and Jay D. Schlueter Ataxia Research Fund. The Center for Magnetic Resonance Research is supported by the National Institute of Biomedical Imaging and Bioengineering (NIBIB) grant P41 EB015894 and the Institutional Center Cores for Advanced Neuroimaging

award P30 NS076408. Research reported in this publication was also supported by the National Center for Advancing Translational Sciences of the National Institutes of Health Award Number UL1TR000114. The content is solely the responsibility of the authors and does not necessarily represent the official views of the National Institutes of Health.

References

1. Miller TM, Pestronk A, David W, et al. An antisense oligonucleotide against SOD1 delivered intrathecally for patients with SOD1 familial amyotrophic lateral sclerosis: a phase 1, randomised, first-in-man study. *Lancet Neurol.* 2013 May; 12(5):435–42. [PubMed: 23541756]
2. Scoto M, Finkel RS, Mercuri E, Muntoni F. Therapeutic approaches for spinal muscular atrophy (SMA). *Gene Ther.* 2017 May 31.doi: 10.1038/gt.2017.45
3. Wild, EJ., Tabrizi, SJ. Premanifest and early Huntington's disease. In: Bates, G.Tabrizi, SJ., Jones, L., editors. *Huntington's Disease.* Oxford, UK: Oxford University Press; 2014.
4. Rubinsztein DC, Orr HT. Diminishing return for mechanistic therapeutics with neurodegenerative disease duration?: There may be a point in the course of a neurodegenerative condition where therapeutics targeting disease-causing mechanisms are futile. *Bioessays.* 2016 Oct; 38(10):977–80. [PubMed: 27479863]
5. Zu T, Duvick LA, Kaytor MD, et al. Recovery from polyglutamine-induced neurodegeneration in conditional SCA1 transgenic mice. *J Neurosci.* 2004 Oct 6; 24(40):8853–61. [PubMed: 15470152]
6. Yamamoto A, Lucas JJ, Hen R. Reversal of neuropathology and motor dysfunction in a conditional model of Huntington's disease. *Cell.* 2000 Mar 31; 101(1):57–66. [PubMed: 10778856]
7. Tabrizi SJ, Reilmann R, Roos RA, et al. Potential endpoints for clinical trials in premanifest and early Huntington's disease in the TRACK-HD study: analysis of 24 month observational data. *Lancet Neurol.* 2012 Jan; 11(1):42–53. [PubMed: 22137354]
8. Jacobi H, Reetz K, du Montcel ST, et al. Biological and clinical characteristics of individuals at risk for spinocerebellar ataxia types 1, 2, 3, and 6 in the longitudinal RISCA study: analysis of baseline data. *Lancet Neurol.* 2013 Jul; 12(7):650–8. [PubMed: 23707147]
9. Paulsen JS, Langbehn DR, Stout JC, et al. Detection of Huntington's disease decades before diagnosis: the Predict-HD study. *J Neurol Neurosurg Psychiatry.* 2008 Aug; 79(8):874–80. [PubMed: 18096682]
10. Öz G, Alger JR, Barker PB, et al. Clinical proton MR spectroscopy in central nervous system disorders. *Radiology.* 2014 Mar; 270(3):658–79. [PubMed: 24568703]
11. Öz G, Hutter D, Tkáč I, et al. Neurochemical alterations in spinocerebellar ataxia type 1 and their correlations with clinical status. *Mov Disord.* 2010; 25(9):1253–61. [PubMed: 20310029]
12. Adanyeguh IM, Henry PG, Nguyen TM, et al. In vivo neurometabolic profiling in patients with spinocerebellar ataxia types 1, 2, 3, and 7. *Mov Disord.* 2015 Apr 15; 30(5):662–70. [PubMed: 25773989]
13. Öz G, Iltis I, Hutter D, Thomas W, Bushara KO, Gomez CM. Distinct Neurochemical Profiles of Spinocerebellar Ataxias 1, 2, 6, and Cerebellar Multiple System Atrophy. *Cerebellum.* 2011 Jun; 10(2):208–17. [PubMed: 20838948]
14. Schöls L, Bauer P, Schmidt T, Schulte T, Riess O. Autosomal dominant cerebellar ataxias: clinical features, genetics, and pathogenesis. *Lancet Neurol.* 2004 May; 3(5):291–304. [PubMed: 15099544]
15. Schmitz-Hübsch T, du Montcel ST, Baliko L, et al. Scale for the assessment and rating of ataxia: development of a new clinical scale. *Neurology.* 2006 Jun 13; 66(11):1717–20. [PubMed: 16769946]
16. Rub U, Schöls L, Paulson H, et al. Clinical features, neurogenetics and neuropathology of the polyglutamine spinocerebellar ataxias type 1, 2, 3, 6 and 7. *Prog Neurobiol.* 2013 May.104:38–66. [PubMed: 23438480]
17. Fiszer A, Olejniczak M, Switonski PM, et al. An evaluation of oligonucleotide-based therapeutic strategies for polyQ diseases. *BMC Mol Biol.* 2012 Mar 07.13:6. [PubMed: 22397573]

18. do Carmo Costa M, Luna-Cancelon K, Fischer S, et al. Toward RNAi Therapy for the Polyglutamine Disease Machado-Joseph Disease. *Mol Ther.* 2013 Oct; 21(10):1898–908. [PubMed: 23765441]
19. Keiser MS, Monteys AM, Corbau R, Gonzalez-Alegre P, Davidson BL. RNAi prevents and reverses phenotypes induced by mutant human ataxin-1. *Ann Neurol.* 2016 Nov; 80(5):754–65. [PubMed: 27686464]
20. Öz G, Nelson CD, Koski DM, et al. Noninvasive detection of presymptomatic and progressive neurodegeneration in a mouse model of spinocerebellar ataxia type 1. *J Neurosci.* 2010 Mar 10; 30(10):3831–8. [PubMed: 20220018]
21. Emir UE, Brent Clark H, Vollmers ML, Eberly LE, Öz G. Non-invasive detection of neurochemical changes prior to overt pathology in a mouse model of spinocerebellar ataxia type 1. *J Neurochem.* 2013 Aug 27; 127(5):660–8. [PubMed: 24032423]
22. Öz G, Vollmers ML, Nelson CD, et al. In vivo monitoring of recovery from neurodegeneration in conditional transgenic SCA1 mice. *Exp Neurol.* 2011 Dec; 232(2):290–8. [PubMed: 21963649]
23. Öz G, Kittelson E, Demirgoz D, et al. Assessing recovery from neurodegeneration in spinocerebellar ataxia 1: Comparison of in vivo magnetic resonance spectroscopy with motor testing, gene expression and histology. *Neurobiol Dis.* 2015 Feb; 74:158–66. [PubMed: 25446943]
24. Marron JS, Todd MJ, Ahn J. Distance-Weighted Discrimination. *J Am Stat Assoc.* 2007; 102(480): 1267–71.
25. Maas RP, van Gaalen J, Klockgether T, van de Warrenburg BP. The preclinical stage of spinocerebellar ataxias. *Neurology.* 2015 Jul 07; 85(1):96–103. [PubMed: 26062625]
26. Pratico D. F(2)-isoprostanes: sensitive and specific non-invasive indices of lipid peroxidation in vivo. *Atherosclerosis.* 1999 Nov 1; 147(1):1–10. [PubMed: 10525118]
27. Hermann D, Sartorius A, Welzel H, et al. Dorsolateral prefrontal cortex N-acetylaspartate/total creatine (NAA/tCr) loss in male recreational cannabis users. *Biol Psychiatry.* 2007 Jun 01; 61(11): 1281–9. [PubMed: 17239356]
28. Schwedhelm E, Maas R, Troost R, Boger RH. Clinical pharmacokinetics of antioxidants and their impact on systemic oxidative stress. *Clin Pharmacokinet.* 2003; 42(5):437–59. [PubMed: 12739983]
29. Shults CW, Beal MF, Song D, Fontaine D. Pilot trial of high dosages of coenzyme Q10 in patients with Parkinson's disease. *Exp Neurol.* 2004 Aug; 188(2):491–4. [PubMed: 15246848]
30. Subramony SH, May W, Lynch D, et al. Measuring Friedreich ataxia: Interrater reliability of a neurologic rating scale. *Neurology.* 2005 Apr 12; 64(7):1261–2. [PubMed: 15824358]
31. Patel M, Isaacs CJ, Seyer L, et al. Progression of Friedreich ataxia: quantitative characterization over 5 years. *Ann Clin Transl Neurol.* 2016 Sep; 3(9):684–94. [PubMed: 27648458]
32. Adriany G, Van de Moortele PF, Ritter J, et al. A geometrically adjustable 16-channel transmit/receive transmission line array for improved RF efficiency and parallel imaging performance at 7 Tesla. *Magn Reson Med.* 2008 Mar; 59(3):590–7. [PubMed: 18219635]
33. Emir UE, Auerbach EJ, Moortele PF, et al. Regional neurochemical profiles in the human brain measured by ¹H MRS at 7 T using local B₁ shimming. *NMR Biomed.* 2012 Jan; 25(1):152–60. [PubMed: 21766380]
34. Metzger GJ, Snyder C, Akgun C, Vaughan T, Ugurbil K, Van de Moortele PF. Local B₁⁺ shimming for prostate imaging with transceiver arrays at 7T based on subject-dependent transmit phase measurements. *Magn Reson Med.* 2008 Feb; 59(2):396–409. [PubMed: 18228604]
35. Öz G, Tká I. Short-echo, single-shot, full-intensity proton magnetic resonance spectroscopy for neurochemical profiling at 4 T: Validation in the cerebellum and brainstem. *Magn Reson Med.* 2011 Apr; 65(4):901–10. [PubMed: 21413056]
36. Deelchand DK, Adanyeguh IM, Emir UE, et al. Two-site reproducibility of cerebellar and brainstem neurochemical profiles with short-echo, single voxel MRS at 3 T. *Magn. Reson Med.* 2015; 73(5):1718–25.
37. Terpstra M, Cheong I, Lyu T, et al. Test-retest reproducibility of neurochemical profiles with short-echo, single-voxel MR spectroscopy at 3T and 7T. *Magn Reson Med.* 2016 Oct; 76(4):1083–91. [PubMed: 26502373]

38. Provencher SW. Estimation of metabolite concentrations from localized in vivo proton NMR spectra. *Magn Reson Med*. 1993 Dec; 30(6):672–9. [PubMed: 8139448]
39. Storm-Mathisen J, Danbolt NC, Rothe F, et al. Ultrastructural immunocytochemical observations on the localization, metabolism and transport of glutamate in normal and ischemic brain tissue. *Prog Brain Res*. 1992; 94:225–41. [PubMed: 1363142]
40. Guerrini L, Belli G, Mazzoni L, et al. Impact of cerebrospinal fluid contamination on brain metabolites evaluation with ¹H-MR spectroscopy: a single voxel study of the cerebellar vermis in patients with degenerative ataxias. *J Magn Reson Imaging*. 2009 Jul; 30(1):11–7. [PubMed: 19557841]
41. Tezenas du Montcel S, Durr A, Rakowicz M, et al. Prediction of the age at onset in spinocerebellar ataxia type 1, 2, 3 and 6. *J Med Genet*. 2014 Jul; 51(7):479–86. [PubMed: 24780882]
42. Reetz K, Costa AS, Mirzazade S, et al. Genotype-specific patterns of atrophy progression are more sensitive than clinical decline in SCA1, SCA3 and SCA6. *Brain*. 2013 Mar; 136(Pt 3):905–17. [PubMed: 23423669]
43. Mascaldi M, Tosetti M, Plasmati R, et al. Proton magnetic resonance spectroscopy in an Italian family with spinocerebellar ataxia type 1. *Ann Neurol*. 1998 Feb; 43(2):244–52. [PubMed: 9485066]
44. Ashizawa T, Figueroa KP, Perlman SL, et al. Clinical characteristics of patients with spinocerebellar ataxias 1, 2, 3 and 6 in the US; a prospective observational study. *Orphanet J Rare Dis*. 2013; 8:177. [PubMed: 24225362]
45. Jacobi H, du Montcel ST, Bauer P, et al. Long-term disease progression in spinocerebellar ataxia types 1, 2, 3, and 6: a longitudinal cohort study. *Lancet Neurol*. 2015 Nov; 14(11):1101–8. [PubMed: 26377379]
46. Koeppe AH. The pathogenesis of spinocerebellar ataxia. *Cerebellum*. 2005; 4(1):62–73. [PubMed: 15895563]
47. Schöls L, Reimold M, Seidel K, et al. No parkinsonism in SCA2 and SCA3 despite severe neurodegeneration of the dopaminergic substantia nigra. *Brain*. 2015 Nov; 138(Pt 11):3316–26. [PubMed: 26362908]
48. Wüllner U, Reimold M, Abele M, et al. Dopamine transporter positron emission tomography in spinocerebellar ataxias type 1, 2, 3, and 6. *Arch Neurol*. 2005 Aug; 62(8):1280–5. [PubMed: 16087769]
49. Koeppe AH, Dickson AC, Lamarche JB, Robitaille Y. Synapses in the hereditary ataxias. *J Neuropathol Exp Neurol*. 1999 Jul; 58(7):748–64. [PubMed: 10411345]
50. van de Bank BL, Emir UE, Boer VO, et al. Multi-center reproducibility of neurochemical profiles in the human brain at 7 T. *NMR Biomed*. 2015 Jan 8; 28(3):306–16. [PubMed: 25581510]

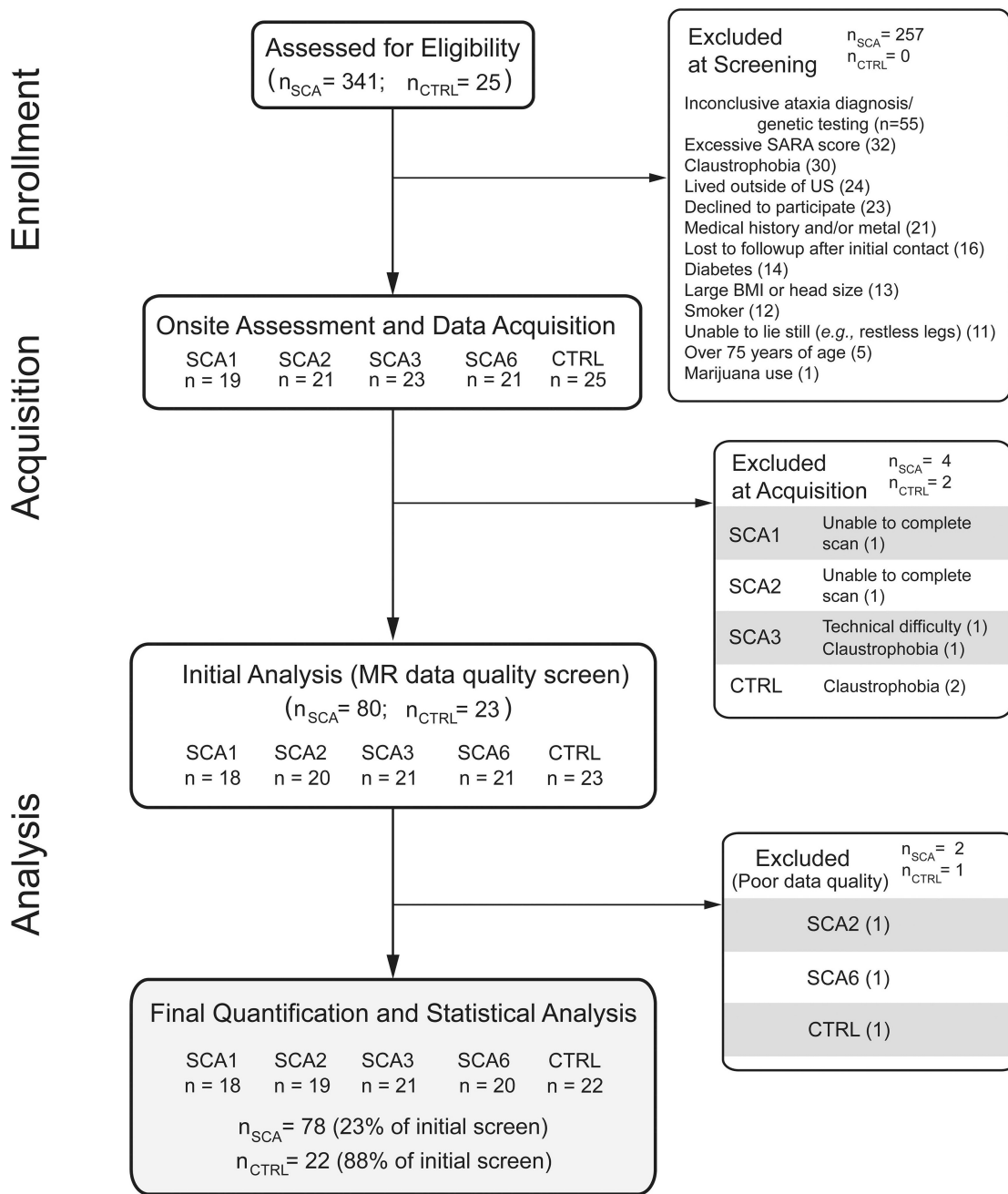


Fig. 1. Flow diagram describing subject enrollment throughout the study
 Screening was performed remotely as described in Methods. The bottom panel shows the number of subjects whose data were used in the final analysis.

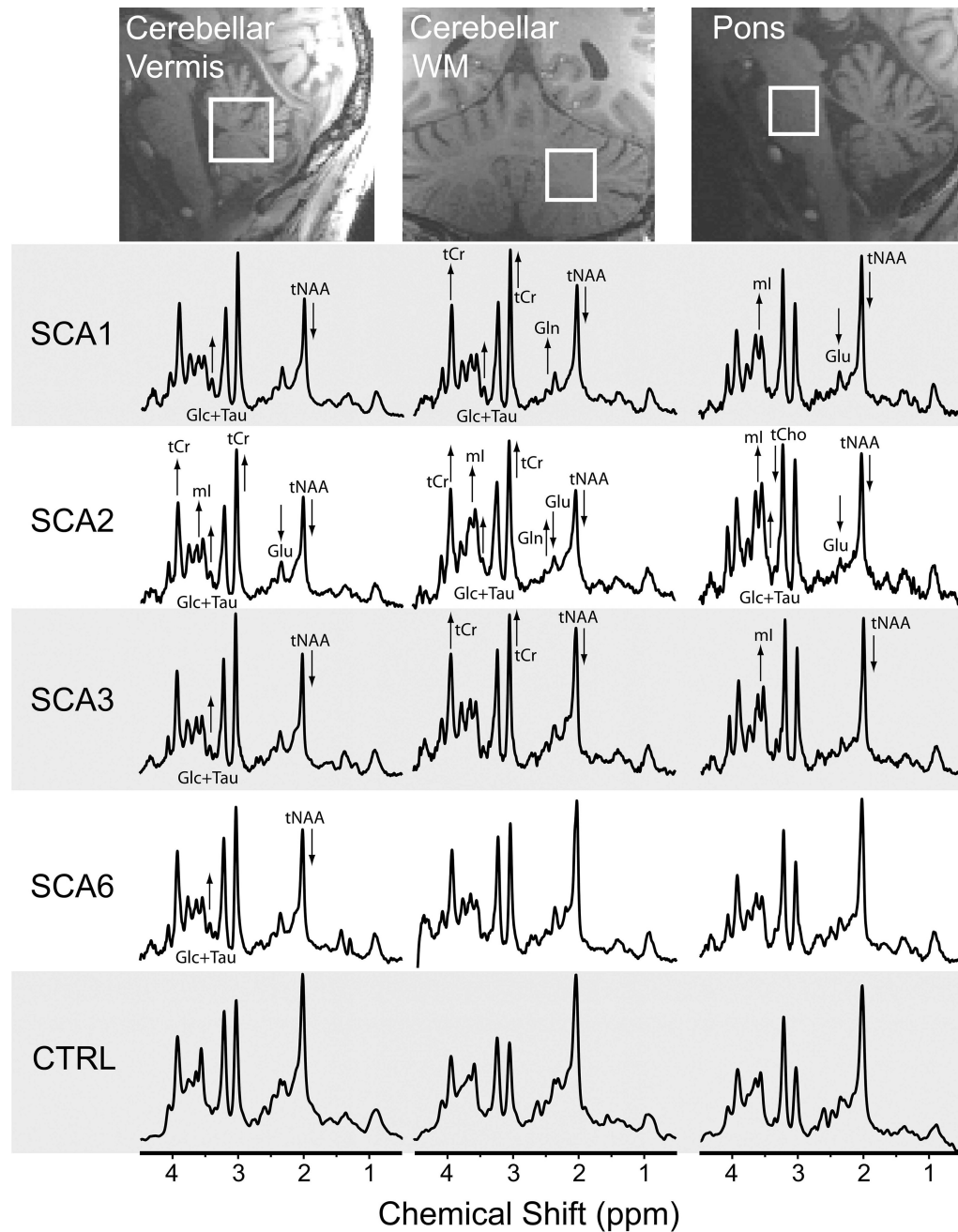


Fig. 2. Detection of neurochemical abnormalities in MR spectra obtained from individuals with SCA at premanifest stage vs. healthy controls

MRS voxel locations and spectra (semi-LASER, TE=26 ms, TR=5 s, 64 transients) are shown from a single subject in each group; subjects with SCAs were at the premanifest stage (SARA = 2.5). Arrows indicate type I error corrected significant group metabolite differences in each early SCA group compared to controls. [Abbreviations: *Glc*, glucose; *Gln*, glutamine; *Glu*, glutamate; *mI*, myo-inositol; *tCho*, total choline; *tCr*, total creatine; *tNAA*, total N-acetylaspartate; *Tau*, taurine].

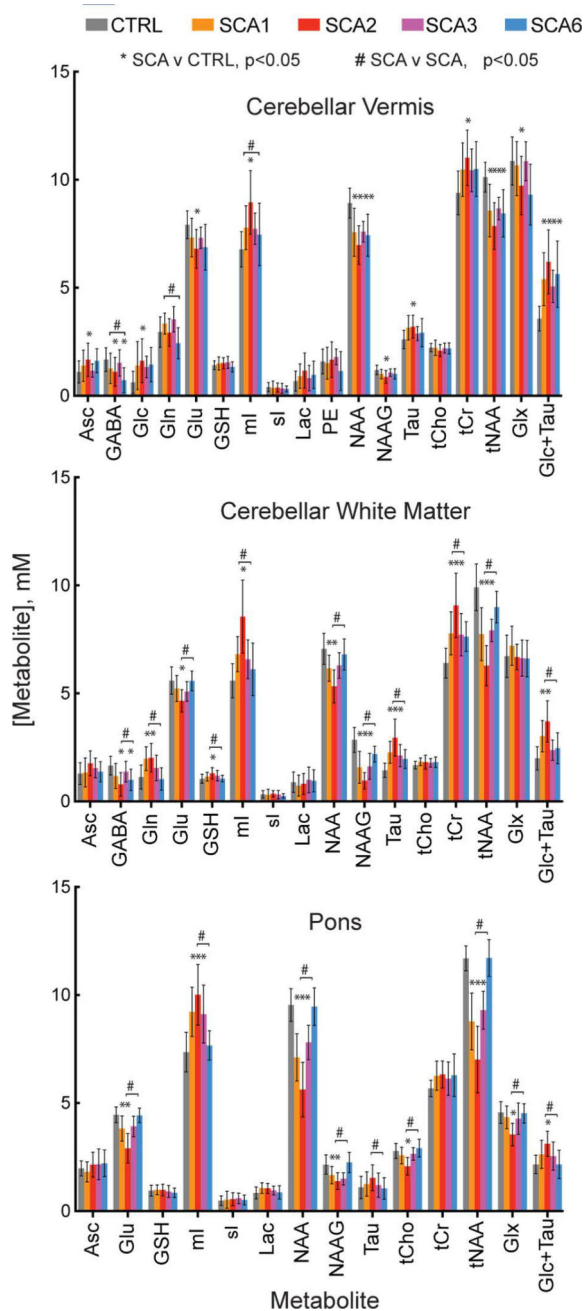


Fig. 3. Regional neurochemical profiles

Neurochemical profiles from each of the subject groups for each of the VOIs. Error bars indicate standard deviation. Only metabolites with mean Cramér-Rao lower bounds (CRLB) 20% in at least one group are included in the profiles. Significant differences ($p < 0.05$, type I error corrected) between SCA and control (*) and between any two SCA types (#) are marked. Sample sizes are listed in Fig. 1 and group differences, confidence intervals, and p -values for all metabolite comparisons are provided in Table S1. [Abbreviations: Asc, ascorbate; GABA, γ -aminobutyric acid; Glc, glucose; Gln, glutamine; Glu, glutamate; GSH, glutathione; mI, myo-inositol; sI, scyllo-inositol; Lac, lactate; NAA, N-acetylaspartate;

NAAG, N-acetylaspartylglutamate; PE, phosphorylethanolamine; Tau, taurine; tCho, total choline; tCr, total creatine; tNAA, NAA+NAAG; Glx, Gln+Glu].

Author Manuscript

Author Manuscript

Author Manuscript

Author Manuscript

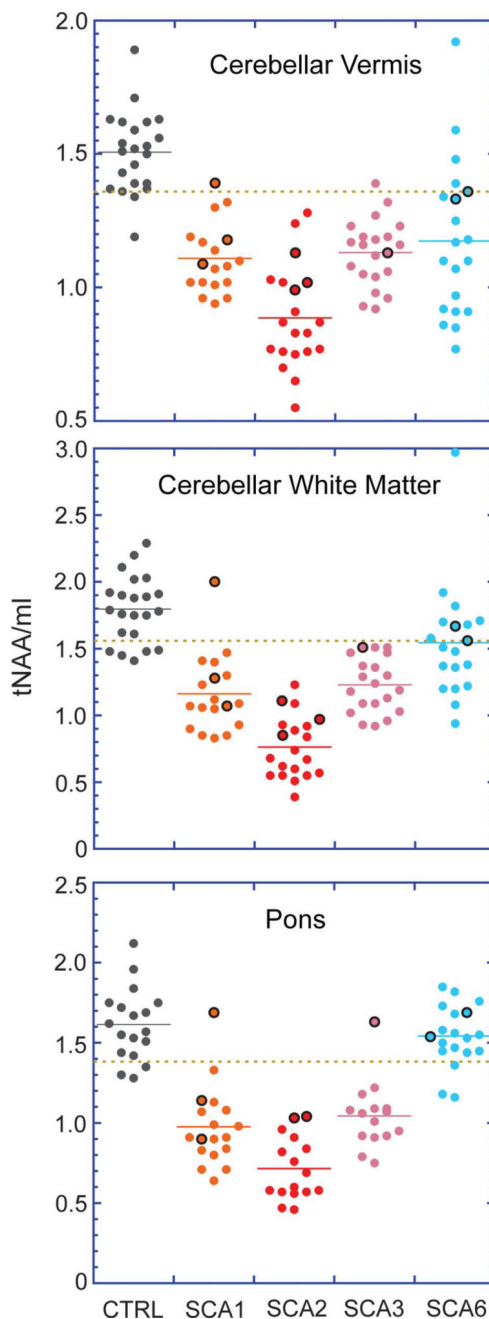


Fig. 4. Total *N* acetylaspartate-to-myoinositol ratios (tNAA/ml) for all subjects
 Data from premanifest subjects (SARA = 2.5) are denoted as points encircled with black. The dashed copper line indicates the mean minus one SD for the control group in each plot. One premanifest SCA1 and two premanifest SCA6 subjects who are within the control mean \pm SD range in all plots are those subjects with estimated ataxia onset more than 10 years away. One of the premanifest SCA2 subjects lacked data from the pons, hence the loss of a data point in the pons plots.

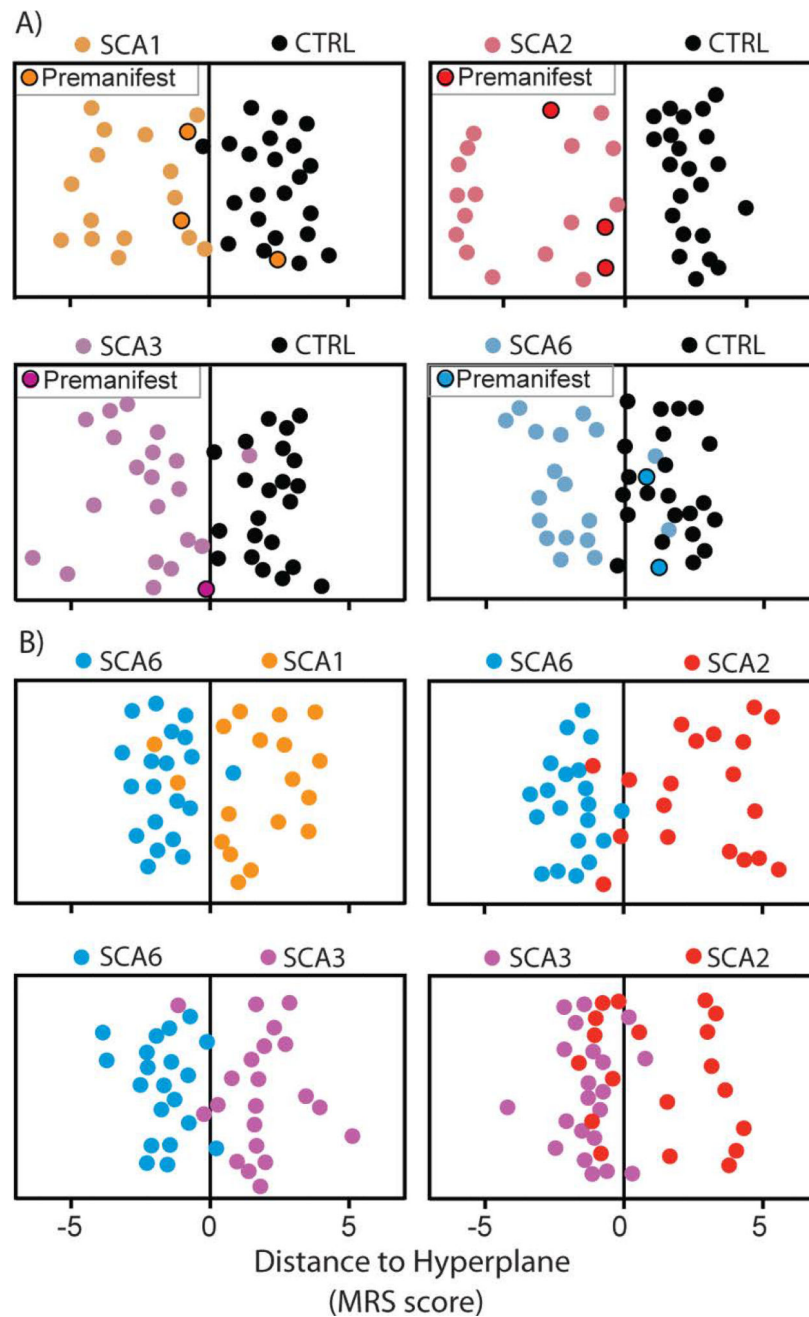


Fig. 5. SCA classification based on distance-weighted discrimination

Distance-weighted discrimination jitter plots of MRS scores from binary group comparisons between **A)** SCA vs healthy controls and **B)** SCA vs SCA. Data points with black borders indicate subjects with SCA who were in the premanifest stage ($SARA < 2.5$). Each subject's MRS score is a projection from 48-dimensional space (each regional metabolite contributes one dimension: $DWDdim_{tot} = dim_{Vermis} + dim_{CWM} + dim_{Pons} = 18+16+14$).

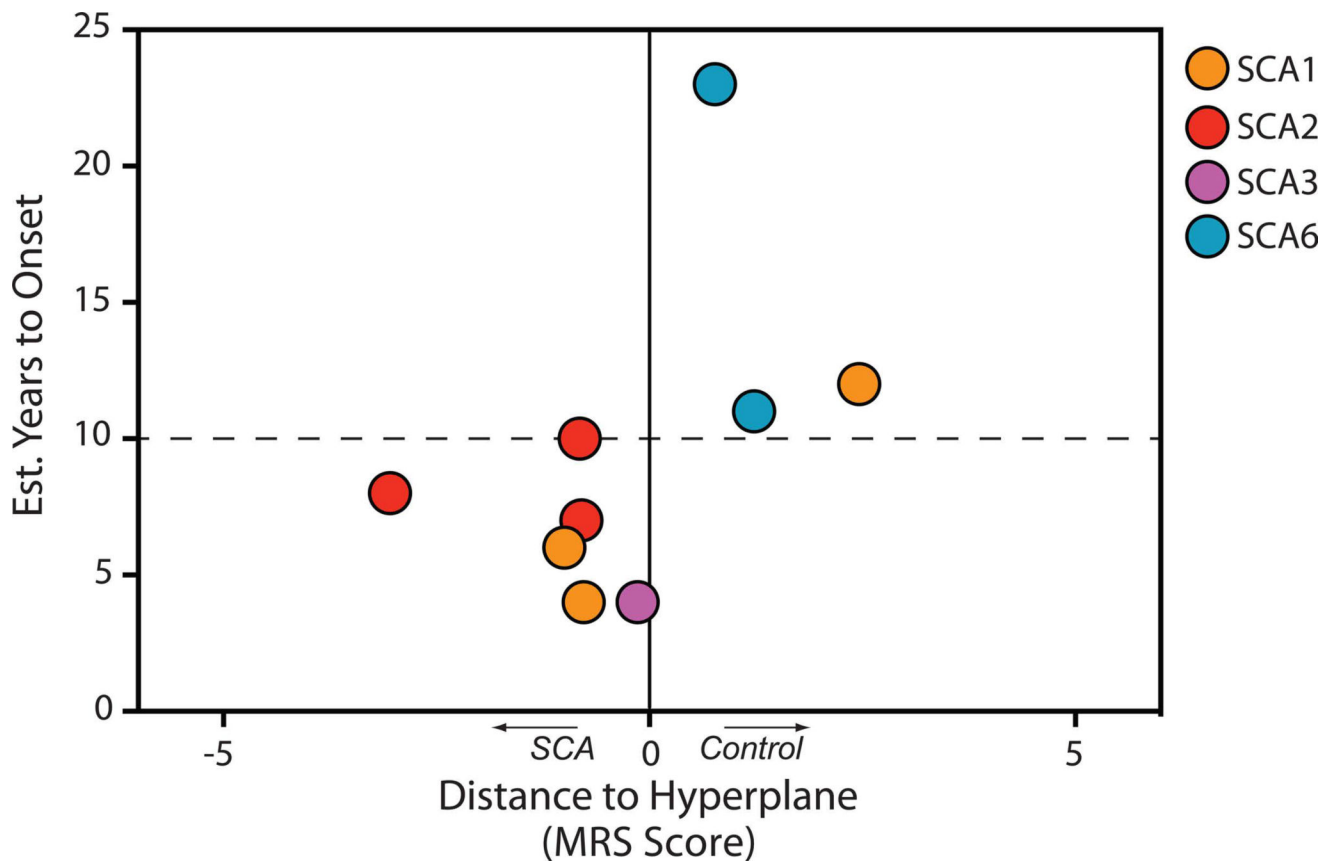


Fig. 6. Detection of neurochemical abnormalities in premanifest subjects in relation to estimated time to ataxia onset

MRS scores were taken from each premanifest (SARA ≥ 2.5) subject's score from the appropriate SCA type vs. healthy control binary DWD analysis.

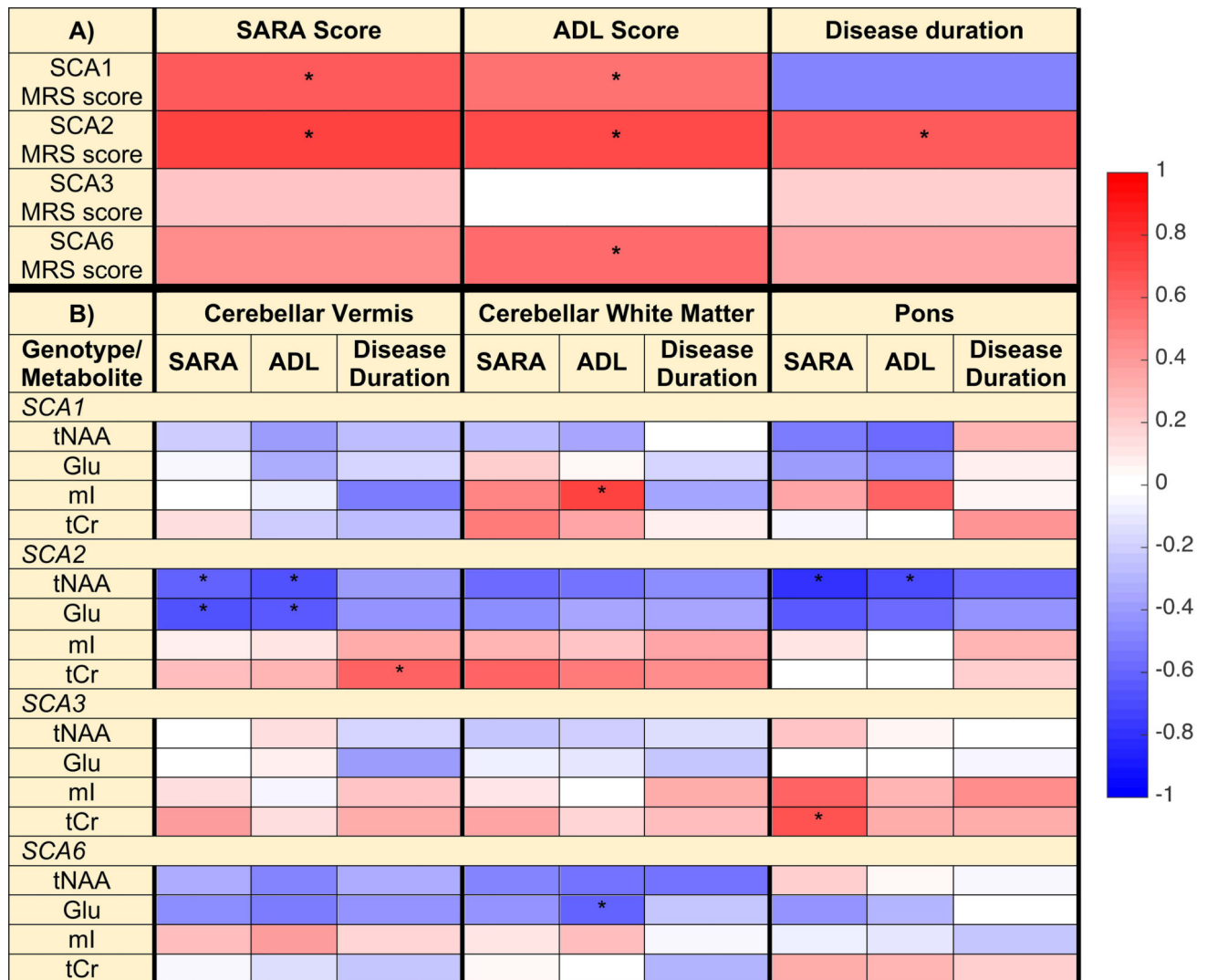


Fig. 7. Pearson correlations between DWD-based MRS scores and clinical measures (A) and between regional metabolite concentrations and clinical measures (B)
Correlations included subjects with SCA only, with MRS scores from DWD models of each SCA type vs. controls; the sign of the MRS scores were reversed so that larger positive scores correspond to being farther from the hyperplane (farther from controls). The heat map and corresponding color bar reflect the magnitude of the correlation coefficients. Correlations with $p < 0.05$ (type I error corrected) are denoted with '*'. Correlations, confidence intervals, and p-values are provided in Tables S2 and S3.

Table 1

Subject demographics and clinical characteristics

| Parameter/metric | SCA1 | SCA2 | SCA3 | SCA6 | CTRL |
|--|------------------------|-------------------------|------------------------|------------------------|------------|
| Sex (F/M) ¹ | 10/8 | 10/9 | 11/10 | 15/5 | 9/13 |
| Age at study enrollment (years) ¹ | 49 ± 11 ^a | 44 ± 11 ^a | 51 ± 11 ^a | 62 ± 10 | 53 ± 16 |
| Age at onset (years) ² | 39 ± 12 ^a | 34 ± 10 ^{a, b} | 44 ± 8 ^a | 53 ± 11 | - |
| Age of diagnosis (years) | 42 ± 12 ^a | 38 ± 11 ^a | 47 ± 13 ^a | 58 ± 11 | - |
| Disease duration (years) ³ | 11 ± 5 | 9 ± 8 | 8 ± 5 | 11 ± 7 | - |
| CAG repeat length ⁴ | 45 ± 3 | 39 ± 3 | 71 ± 4 | 22 ± 1 | - |
| SARA score ⁵ | 8.3 ± 4.0 ^c | 9.5 ± 6.8 ^c | 7.1 ± 2.9 ^c | 9.8 ± 6.5 ^c | 0.1 ± 0.2 |
| ADL score ⁵ | 5.9 ± 4.0 ^c | 6.2 ± 5.5 ^c | 5.2 ± 3.3 ^c | 7.9 ± 6.3 ^c | 0.0 ± 0.0 |
| BMI (kg/m ²) ⁶ | 26.5 ± 3.5 | 25.9 ± 4.0 | 25.0 ± 2.4 | 27.0 ± 4.3 | 25.8 ± 5.1 |

Reported values are mean ± SD

¹No significant differences in sex and age were observed for SCA groups vs. the healthy control group and in sex between the SCA groups.²Mean age at onset for subjects with manifest ataxia (SARA > 2.5). Value is a self-reported estimate based on memory of perceived ataxia onset.³Disease duration is the difference between age at enrollment and the self-reported age of onset for subjects with manifest disease. Disease duration was not significantly different among SCA groups.⁴Number of triplet repeats in the expanded allele⁵Scale for the Assessment and Rating of Ataxia (SARA) and activities of daily living (ADL) scores were not significantly different among SCA groups.⁶No significant body mass index (BMI) difference was observed among all groups.^ap<0.05 for each of SCA1, SCA2 and SCA3 vs. SCA6.^bp<0.05 for SCA2 vs. SCA3.^cp<0.002 for SCA vs. healthy controls.